Scientific Research Publishing

International Journal of Astronomy and Astrophysics, 2026, 16(2), 61-78
https://www.scirp.org/journal/ijaa
ISSN Online: 2161-4725
ISSN Print: 2161-4717

Transport in Astrophysics: VIII. Cosmic Ray Acceleration in the Solar Corona

Lorenzo Zaninetti

Department of Physics, University of Turin, Turin, Italy
Email: l.zaninetti@alice.it

How to cite this paper: Zaninetti, L. (2026) Transport in Astrophysics: VIII. Cosmic Ray Acceleration in the Solar Corona. *International Journal of Astronomy and Astrophysics*, **16**, 61-78.
https://doi.org/10.4236/ijaa.2026.162005

Received: February 8, 2026
Accepted: May 25, 2026
Published: May 28, 2026

Abstract

We derive the acceleration, velocity and distance of a cosmic ray (CR) due to an astrophysical electric field in the framework of special relativity. The relation between distance and time has been inverted, which allows expressing the velocity as a function of the distance. A simulation is performed for the observed spectrum of CRs adopting two distributions for them: the Maxwell Jüttner distribution and the gamma-Pareto II distribution.

Keywords

Cosmic Rays, Particle Acceleration

1. Introduction

In order to explain the non-thermal behaviour of protons and electrons in many astrophysical contexts, the particles should be accelerated. At the moment of writing, there are many theoretical mechanisms for the acceleration; we select some of them. The first one is stochastic and is due to Fermi in 1954. The gain in energy in a continuous form for a particle which spirals around a line of force [1] [2], is proportional to its energy, E,

$$\frac{\mathrm{d}E}{\mathrm{d}t} = \frac{E}{\tau_{II}}, \tag{1}$$

where τ_{II} is the typical time-scale,

$$\frac{1}{\tau_{II}} = \frac{4}{3}\left(\frac{u^2}{c^2}\right)\left(\frac{c}{L_{II}}\right), \tag{2}$$

where u is the speed of the accelerating cloud, c is the speed of light, and L_{II} is the mean free path between clouds, see Equation 4.439 in [3]. Parker in 1955 investigated the hydrodynamic and hydro-magnetic equations from the viewpoint

of energy propagation [4]. Interactions, not considered by Fermi, in which the average energy change is zero may contribute much, or all, of the acceleration [5]. The consideration of the generation of cosmic rays (CRs) by ion plasma turbulence began with Tsytovich [6]. Some improvements of the Fermi acceleration connected with the possibility of creating a wide variety of energy- or rigidity-dependent spectra were analysed [7]. Two possibilities for models of CRs were analysed: the concomitant acceleration and propagation (CAP) model and the sequential acceleration and propagation (SAP) model [8]. The efficiency of diffusive acceleration in shock waves has been evaluated [9]. A numerical treatment of the plasma-physical injection model at a strong quasi-parallel shock has been devised and incorporated into the combined gas dynamics and the CR diffusion–convection code [10]. Gamma-Ray Bursts are good candidates for the "bottom up" scenario for the generation of the Ultra High Energy (UHE) CRs in the framework of the complementary acceleration downstream of the external shock [11]. The acceleration of solar cosmic rays (SCRs) by the shock waves produced by coronal mass ejections has been explored [12]. An accelerated particle spectrum is derived by integrating the exact particle trajectories in a turbulent magnetic field near the shock [13]. The role played by the initial clumping of ejecta and by the efficient acceleration of CRs in determining the density structure of the post-shock region of a Type Ia supernova remnant (SNR) has been analysed [14]. Proton acceleration in a flare occurs along a singular line of the current sheet by the Lorentz electric field, as in pinch gas discharge [15]. A spectrum of the protons produced by a fast shock with a speed of 5000 km s^{-1} in the lower solar corona has been analysed [16].

The previous approaches leave some questions unanswered.

1) Is it possible to accelerate the CRs in an astrophysical electric field?

2) Is it possible to fix the astrophysical parameters in order to have acceleration of the CRs in the region between one solar radius and 1/10 of an astronomical unit (AU)?

3) Does the acceleration affect the entire energy spectrum or only the energies lower than one GeV?

In order to answer the above questions, we derive, in Section 2, the distance, velocity and acceleration of a particle in the presence of a constant electric field in the framework of special relativity. Section 3 reviews two distributions for the initial energy of CRs and then presents the results of the acceleration. Section 4 reviews useful astrophysical parameters in the solar flares and solar corona.

2. Acceleration of Cosmic Rays

In classical mechanics, motion is modeled by Newton's Second Law:

$$\vec{F} = m\vec{a}, \tag{3}$$

where $\vec{F}$ is the force, m is the mass and $\vec{a}$ is the acceleration. An example of the trajectory, $x(t)$, in the presence of a constant force along the X-axis is,

$$x(t) = \frac{Ft^2}{2m}. \tag{4}$$

In special relativity the equation of motion is

$$\vec{F} = \frac{\mathrm{d}\vec{p}}{\mathrm{d}t}, \tag{5}$$

where $\vec{F}$ is the force acting on the point with momentum $\vec{p}$ which is

$$p = \gamma m\vec{u}, \tag{6}$$

where m is the rest mass, $\vec{u}$ the velocity and

$$\gamma = \frac{1}{\sqrt{1-\frac{u^2}{c^2}}}, \tag{7}$$

with c being the speed of light. We now analyse the case of a single cosmic ray with mass $A \times m$ where A is the mass number (protons + neutrons) and m is the mass of the proton. In the presence of a constant force, F, in 1D which will be later specified, we integrate the equation of motion (5)

$$\frac{Amu}{\sqrt{1-\frac{u^2}{c^2}}} - \frac{Amu_0}{\sqrt{1-\frac{u_0^2}{c^2}}} = F\left(t-t_0\right), \tag{8}$$

where u_0 is the velocity at $t = t_0$ which can also be parametrized as $u_0 = \beta_0 c$ with $\beta_0 = \frac{u_0}{c}$.

The positive solution for the velocity is

$$u(t) = \frac{c\left(F\left(t-t_0\right)\sqrt{c^2-u_0^2} + Amu_0 c\right)}{\sqrt{2AFcmu_0\left(t-t_0\right)\sqrt{c^2-u_0^2} + \left(t-t_0\right)^2\left(c-u_0\right)\left(c+u_0\right)F^2 + A^2c^4m^2}}, \tag{9}$$

the acceleration, $a(t)$, is

$$a(t) = \frac{c^3FA^2m^2\left(c^2-u_0^2\right)^{3/2}}{\left(2AFcmu_0\left(t-t_0\right)\sqrt{c^2-u_0^2} + \left(t-t_0\right)^2\left(c-u_0\right)\left(c+u_0\right)F^2 + A^2c^4m^2\right)^{3/2}}, \tag{10}$$

the space, $x(t)$, is

$$x(t) = \frac{1}{\sqrt{c^2-u_0^2}\,F} \times \left(-Ac^3m + x_0\sqrt{c^2-u_0^2}F + \sqrt{\begin{array}{l} 2AFcmu_0\left(t-t_0\right)\sqrt{c^2-u_0^2} + \\ \left(t-t_0\right)^2\left(c-u_0\right)\left(c+u_0\right)F^2 + A^2c^4m^2 \end{array}}\, c \right), \tag{11}$$

and the time as a function of the distance, $t(x)$, is

$$t(x) = \frac{1}{Fc\left(c^2-u_0^2\right)} \times \left(-A\sqrt{c^2-u_0^2}c^2mu_0 + Fc^3t_0 - Fct_0u_0^2 + \frac{\sqrt{2AFc^3m\left(-x_0+x\right)\sqrt{c^2-u_0^2} + \left(-x_0+x\right)^2\left(c-u_0\right)\left(c+u_0\right)F^2 + A^2c^4m^2u_0^2}}{\sqrt{c^2-u_0^2}} \right). \tag{12}$$

We now insert the force due to the electric field, E,

$$E(t) = ZeE, \tag{13}$$

where Z is the charge number and e the elementary charge. The velocity as a function of time in the presence of a constant electric field is

$$u_E(t) = \frac{\left(ZeE(t-t_0)\sqrt{c^2-u_0^2} + Amu_0c\right)c}{\sqrt{\begin{array}{l}2AZeEcmu_0(t-t_0)\sqrt{c^2-u_0^2} + \\ (t-t_0)^2(c-u_0)(c+u_0)Z^2e^2E^2 + A^2c^4m^2\end{array}}}, \tag{14}$$

the acceleration as a function of time is

$$a_E(t) = \frac{ZeEc^3A^2m^2\left(c^2-u_0^2\right)^{3/2}}{\left(\begin{array}{l}2AZeEcmu_0(t-t_0)\sqrt{c^2-u_0^2} + \\ (t-t_0)^2(c-u_0)(c+u_0)Z^2e^2E^2 + A^2c^4m^2\end{array}\right)^{3/2}}, \tag{15}$$

the position as a function of time is

$$x_E(t) = \frac{1}{\sqrt{c^2-u_0^2}\,ZeE} \times \left(-c\left(Ac^2m - \sqrt{\begin{array}{l}2AZeEcmu_0(t-t_0)\sqrt{c^2-u_0^2} + \\ (t-t_0)^2(c-u_0)(c+u_0)Z^2e^2E^2 + A^2c^4m^2\end{array}}\right)\right) + x_0, \tag{16}$$

and the velocity as a function of the position is

$$v(x) = \frac{c\sqrt{\begin{array}{l}2AEZc^3em(x-x_0)\sqrt{c^2-u_0^2} + \\ Z^2e^2(x-x_0)^2(c-u_0)(c+u_0)E^2 + A^2c^4m^2u_0^2\end{array}}}{\sqrt{\begin{array}{l}2AEZc^3em(x-x_0)\sqrt{c^2-u_0^2} + \\ Z^2e^2(x-x_0)^2(c-u_0)(c+u_0)E^2 + A^2c^6m^2\end{array}}}. \tag{17}$$

The final velocity can also be encapsulated in the final γ factor and turns out to be

$$\gamma(t) = \frac{1}{Acm\sqrt{\dfrac{1}{2AEZcem(t-t_0)\sqrt{\gamma_0^2-1} + E^2Z^2e^2(t-t_0)^2 + A^2c^2m^2\gamma_0^2}}}. \tag{18}$$

The relativistic kinetic energy is

$$E_{kin} = mc^2(\gamma - 1), \tag{19}$$

and therefore

$$E_{kin}(t) = mc^2\left(\frac{1}{Acm\sqrt{\dfrac{1}{2AEZcem(t-t_0)\sqrt{\gamma_0^2-1} + Z^2e^2E^2(t-t_0)^2 + A^2c^2m^2\gamma_0^2}}} - 1\right). \tag{20}$$

The above equation are based on the velocity as a function of time and position but in the forthcoming applications to the CRs we will deal with the Lorentz factor

γ and energy E_{CR} expressed in eV. Table 1 presents some useful conversions and their inversions.

Table 1. Conversions and their inverses.

$\beta = \frac{u}{c}$	$u = \beta c$
$\gamma = \frac{1}{\sqrt{1-\frac{u^2}{c^2}}}$	$u = \frac{\sqrt{\gamma^2 - 1}\, c}{\gamma}$
$\gamma_0 = \frac{1}{\sqrt{1-\frac{u_0^2}{c^2}}}$	$u_0 = \frac{\sqrt{\gamma_0^2 - 1}\, c}{\gamma_0}$
$\gamma = 1.06578 E_{kin}(\text{GeV}) + 1$	$E_{kin}(\text{GeV}) = 0.938272\gamma - 0.938272$

An example is given in Figure 1, which presents the increase in the velocity as a function of time with a constant electric field, parameters as in Table 2.

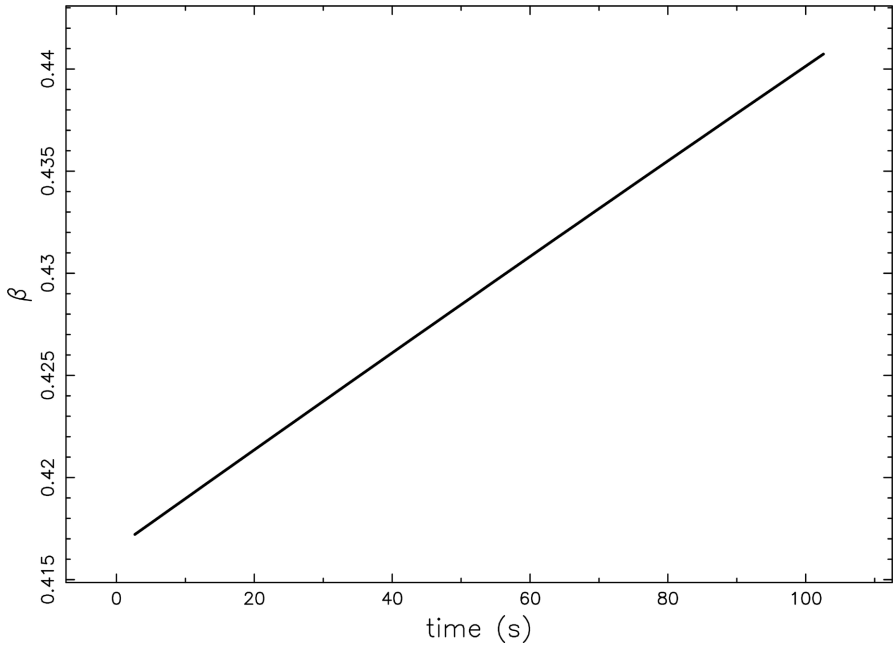

Figure 1. β as function of time with parameters in Table 2.

Table 2. Adopted parameters.

Name	Value	Units
speed of light	$c = 299792458$	m s^{-1}
proton mass	$m = 1.67262192595 \times 10^{-27}$	kg
elementary charge	$e = 1.602176634 \times 10^{-19}$	C

Continued

astronomical unit	$AU = 1.495978707 \times 10^{11}$	m
solar radius	$R_{\odot} = 6.957 \times 10^{8}$	m
Electric field	$E = 1 \times 10^{-3}$	Vm^{-1}
starting point	$x_0 = 1$	$R_{\odot}$
starting velocity	$\beta_0 = 0.416$	number
mass number	$A = 1$	number
charge number	$Z = 1$	number

An energy equivalent in GeV of the above figure is displayed in Figure 2; the adopted conversion is given in Table 1.

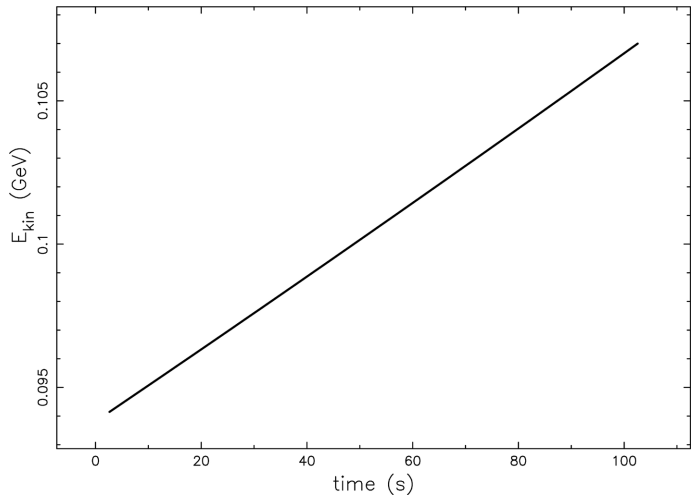

Figure 2. Energy, E_{kin}, as function of time with parameters in Table 2.

The position, expressed in au, as a function of time is shown in Figure 3.

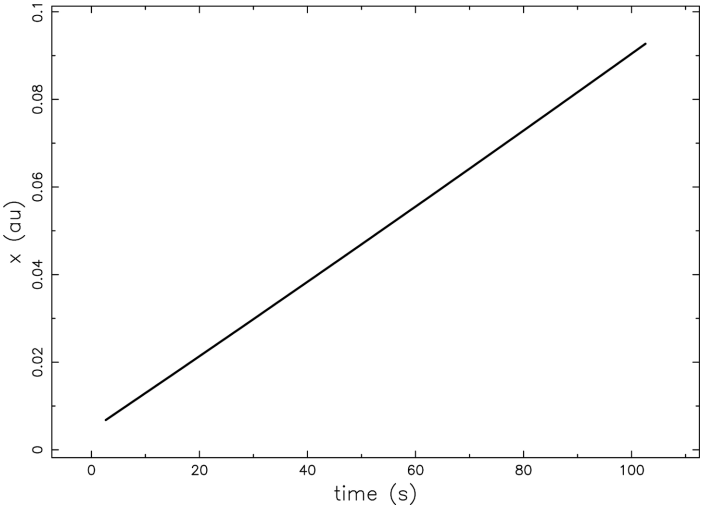

Figure 3. Distance in au as function of time with parameters in Table 2.

3. The Simulation

We now simulate the evolution of the spectrum of CRs in the framework of two probability distributions. The *first* distribution is the Maxwell Jüttner distribution, which extends the Maxwell-Boltzmann distribution to the relativistic regime. The *second* distribution is the gamma-Pareto II, which presents a thermal regime at low energies of the CRs and a power law behaviour at high energies.

3.1. The Maxwell Jüttner Distribution

The PDF for the Maxwell Jüttner (MJ) distribution is

$$f_{MJ}(\gamma;\Theta)=\frac{\gamma\sqrt{\gamma^2-1}\,\mathrm{e}^{-\frac{\gamma}{\Theta}}}{\Theta K_2\left(\frac{1}{\Theta}\right)}, \tag{21}$$

where $\Theta=\sqrt{\frac{kT_{MB}}{mc^2}}$, m is the mass of the gas molecules, k is the Boltzmann constant, T_{MB} is the usual thermodynamic temperature and $K_2(x)$ is the Bessel function of second kind, see [17]-[20]. Its average value is

$$\mu(\Theta)=\frac{-2\Theta^2 G_{1,3}^{2,1}\left(\frac{1}{4\Theta^2}\middle|_{3/2,-1/2,-2}^{1}\right)}{K_2\left(\frac{1}{\Theta}\right)} \tag{22}$$

and its variance is

$$\sigma^2(\Theta)=\frac{1}{\Theta^2\left(K_2\left(\frac{1}{\Theta}\right)\right)^2}\left(-4\Theta^5\left(2K_1\left(\Theta^{-1}\right)G_{1,3}^{2,1}\left(1/4\,\Theta^{-2}\middle|_{5/2,-1/2,-2}^{1}\right)\Theta\right.\right. \tag{23}$$
$$\left.\left.+\left(G_{1,3}^{2,1}\left(1/4\,\Theta^{-2}\middle|_{3/2,-1/2,2}^{1}\right)\right)^2\Theta+K_0\left(\Theta^{-1}\right)G_{1,3}^{2,1}\left(1/4\,\Theta^{-2}\middle|_{5/2,-1/2,2}^{1}\right)\right)\right).$$

The mode can be found by solving the following cubic equation

$$\frac{\mathrm{d}}{\mathrm{d}\gamma}f_{MJ}(\gamma;\Theta)\propto-\gamma^3+2\Theta\gamma^2+\gamma-\Theta=0. \tag{24}$$

The real solution is

$$mode=\frac{1}{6\sqrt[3]{-36\Theta+64\Theta^3+12\sqrt{-96\Theta^4-39\Theta^2-12}}} \tag{25}$$
$$\times\left(\left(-36\Theta+64\Theta^3+12\sqrt{-96\Theta^4-39\Theta^2-12}\right)^{\frac{2}{3}}\right.$$
$$\left.+4\Theta\sqrt[3]{-36\Theta+64\Theta^3+12\sqrt{-96\Theta^4-39\Theta^2-12}}+16\Theta^2+12\right).$$

The above formula allows deriving the parameter Θ when the position of the mode γ_m is given

$$\Theta = \frac{\gamma_m \left(\gamma_m^2 - 1\right)}{2\gamma_m^2 - 1}. \tag{26}$$

More details on the MJ distribution can be found in [21]. An application can be found in the distribution of the hydrogen (H) as observed by PAMELA [22] in the range [0.2,1.2] GeV for the period [2006-07-07, 2007-12-31], see **Figure 4** [22]. A typical example of the MJ distribution applied to the CRs is presented in **Figure 5**.

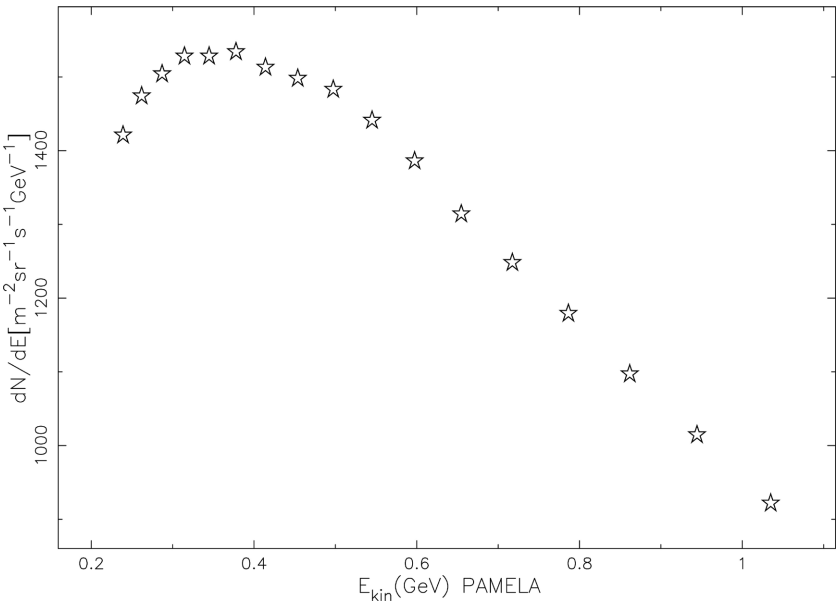

Figure 4. Energy Spectrum versus kinetic energy in GeV as given by PAMELA during seventeen months of observations.

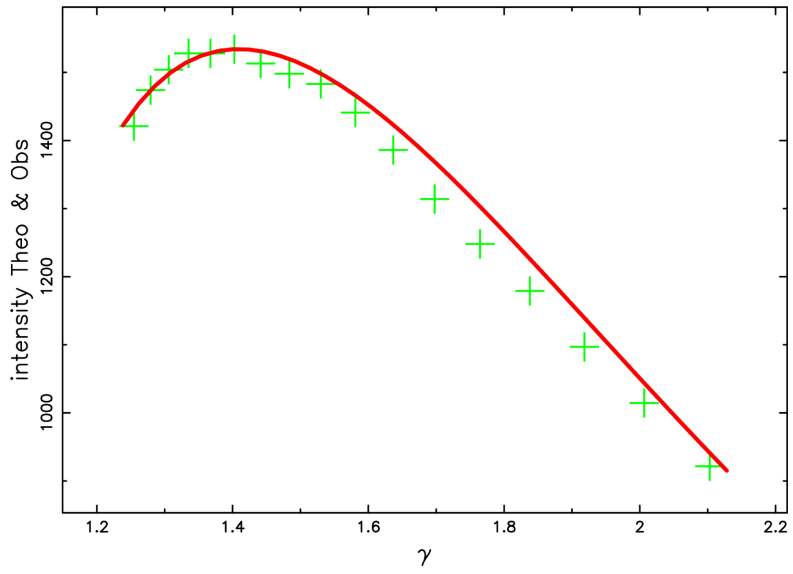

Figure 5. Spectrum of CRs versus the Lorentz factor, γ, as given by PAMELA [22] during seventeen months of observations (green crosses) and the theoretical fit with the M-J distribution (red line) when $\Theta = 0.45$; other parameters as in **Table 2**.

We are now ready to display the evolution of the MJ distribution adopting the following rules:

1) We select an initial γ_0, the Lorentz factor.

2) We convert it in an initial velocity, u_0, according to Table 1.

3) We evaluate the final velocity, u, after a given time (t). according to Equation (14).

4.) We convert the final velocity in the final Lorentz factor, γ, according to Table 1.

5) We restart from point 1 with a bigger value of γ_0.

6) The simulation ends when a significant number of γ_0 belonging to the MJ distribution have been processed.

As an example Figure 6 shows the overall behaviour of the initial spectrum in γ_0, the final spectrum in γ and that observed for PAMELA CRs as a function of γ rather than energy.

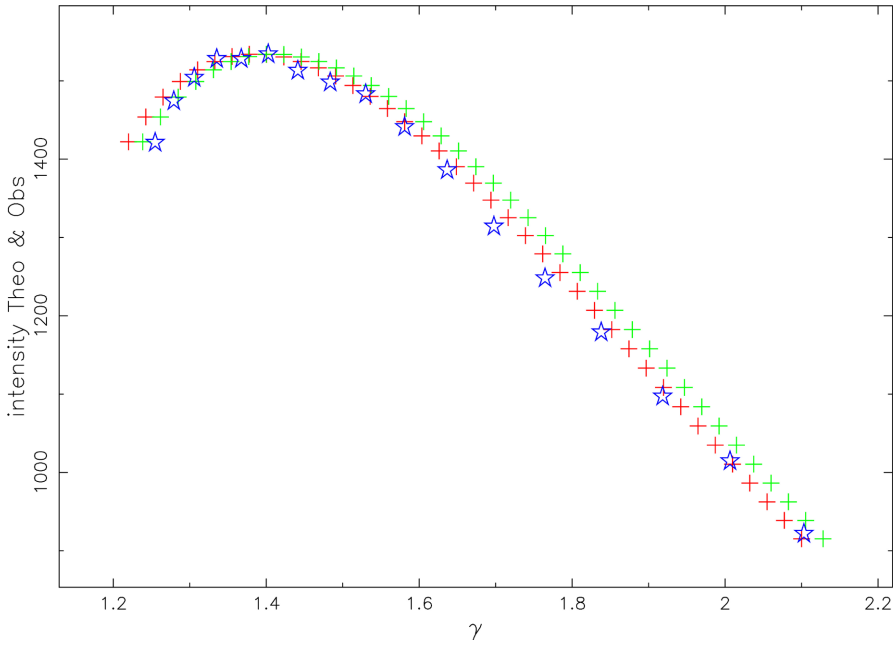

Figure 6. Spectrum of CRs versus the Lorentz factor, γ, as given by PAMELA [22] during seventeen months of observations (blue empty stars), initial values of the Lorentz factor (red crosses) which follow an MJ distribution with $\Theta = 0.45$ and values of the Lorentz factor after the acceleration (green crosses) with parameters as in Table 2.

3.2. The Gamma-Pareto II Distribution

The gamma-Pareto II PDF is

$$f(x;\alpha,c,\theta) = \frac{\theta^{\frac{1}{c}}(x+\theta)^{-1-\frac{1}{c}}\ln\left(1+\frac{x}{\theta}\right)^{\alpha-1}}{c^{\alpha}\Gamma(\alpha)}, \tag{27}$$

which is defined for $\alpha > 0$, $c > 0$, $\theta > 0$ and $x > 0$, see formula (2.4) in Table 1 of [23]. Its average value is

$$\mu(\alpha,c,\theta)=\theta\left((1-c)^{-\alpha}-1\right), \tag{28}$$

and the mode is at

$$Mode(\alpha,c,\theta)=\theta\left(e^{\frac{c(\alpha-1)}{c+1}}-1\right). \tag{29}$$

An application can be found in the distribution of the protons as observed by PAMELA [24] in the range [0.44,1009] GeV, see Figure 7.

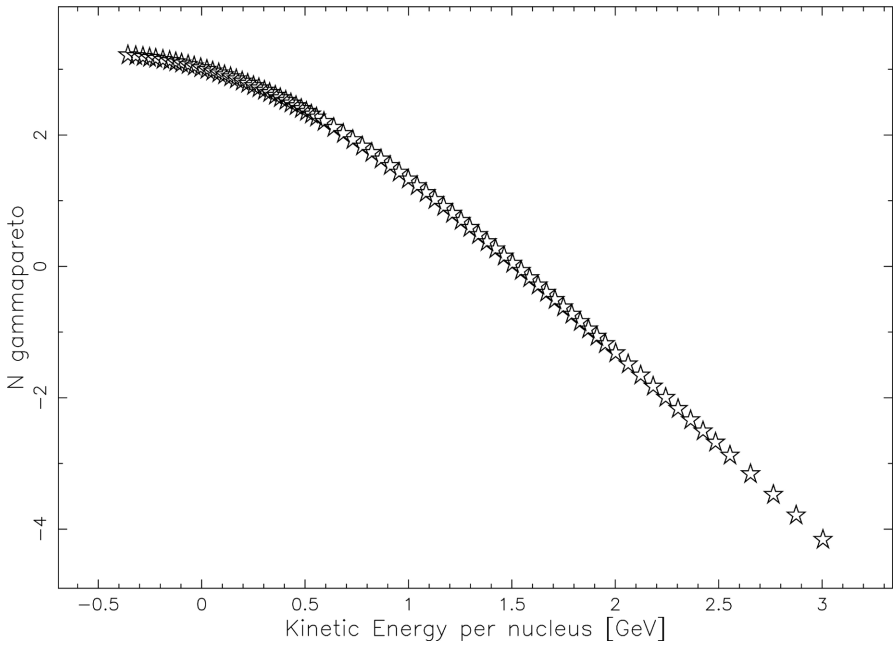

Figure 7. Energy Spectrum of protons versus kinetic energy in GeV as given by PAMELA [24].

Figure 8 presents the fit of the above distribution in energy of CRs with the gamma-Pareto II PDF. We now follow the evolution of the gamma-Pareto II distribution adopting the following rules.

1) We select an initial E_{kin} expressed in GeV.

2) We convert it in γ_0, the Lorentz factor.

3) We convert it in an initial velocity, u_0, according to Table 1.

4) We evaluate the final velocity, u, after a given time (t). according to Equation (14).

5) We convert the final velocity in the final E_{kin}, according to Table 1.

6) We restart from point 1 with a bigger value of E_{kin}.

7) The simulation ends when a significant number of E_{kin} belonging to the gamma-Pareto II distribution have been processed.

As an example, Figure 9 presents the overall behaviour of the initial spectrum in E_{kin}, the final spectrum in E_{kin} and the observed one for PAMELA's CRs as functions of E_{kin}.

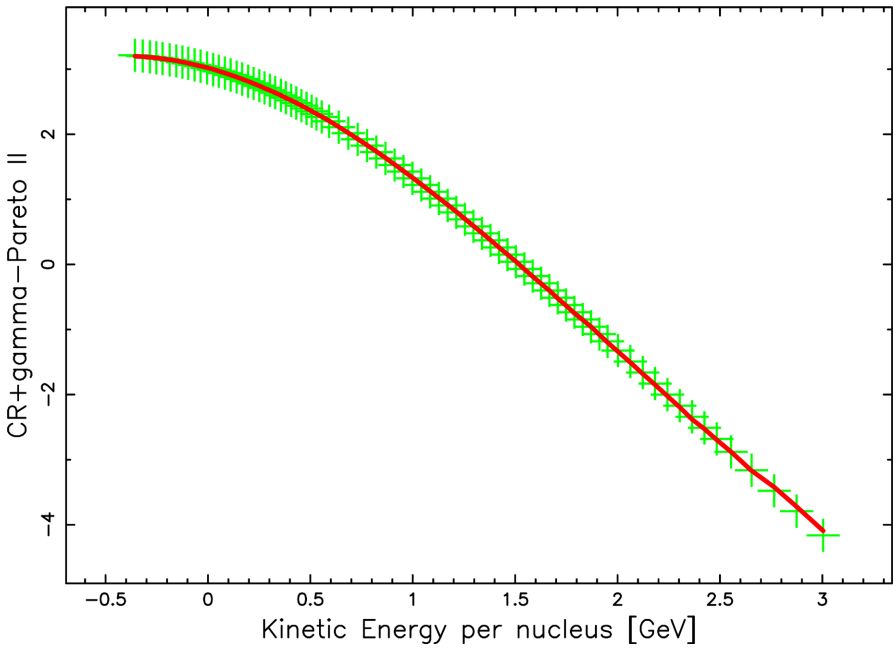

Figure 8. Energy Spectrum of protons versus kinetic energy in GeV as given by PAMELA [24]. The green crosses represent the data of CR and the full red line represents the fit with the gamma-Pareto II PDF when $\theta = 1.469$, $c = 0.517$ and $\alpha = 1.436$.

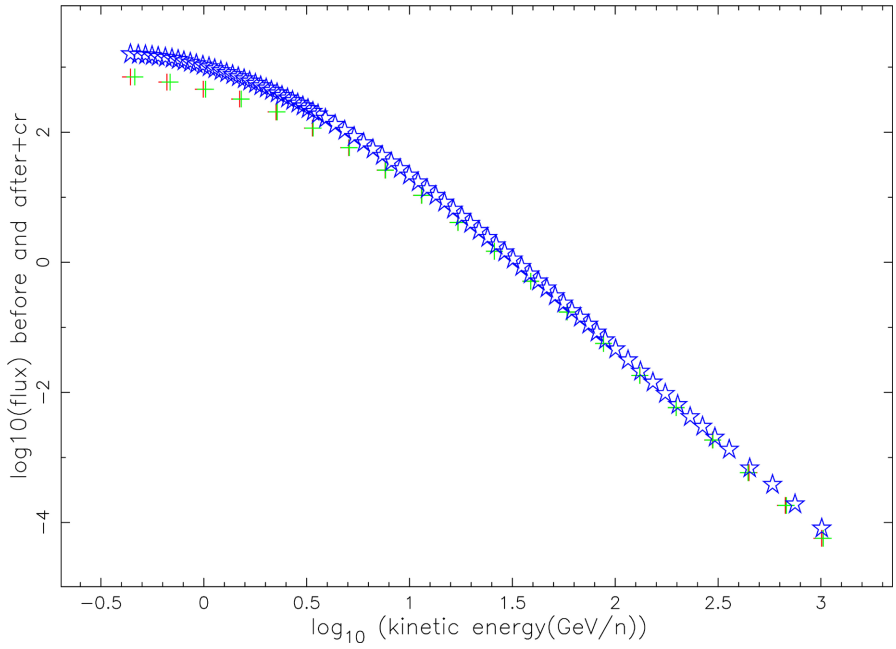

Figure 9. Energy Spectrum of protons versus kinetic energy in GeV as given by PAMELA (blue empty stars), initial values of the kinetic energy (red crosses) which follow a gamma-Pareto II distribution with parameters as in **Figure 8** and final values of the kinetic energy after the acceleration (green crosses) with parameters as in **Table 2**.

A careful analysis of the above Figure reveals that the amount in the acceleration of energy decreases with increasing energy. The diminution of the accelerating effect as function of the increasing energy can be modeled introducing the

percentage error, δ,

$$\delta = \frac{E_{kin}(\text{GeV}) - E_{kin,0}(\text{GeV})}{E_{kin,0}} \times 100. \tag{30}$$

Figure 10 displays such diminution for the acceleration effect.

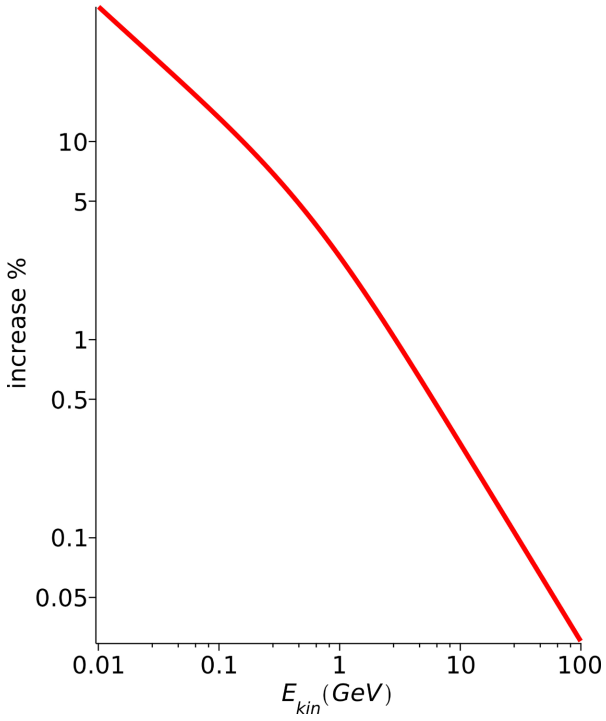

Figure 10. Behaviour of the accelerating effect as function of the energy expressed in GeV.

4. Solar Flares

This section reviews the lognormal distribution, the observations of the solar flares, the electric field and some of the mechanism of acceleration for CRs.

4.1. The Lognormal Distribution

Let X be a random variable taking values x in the interval $[0,\infty]$; the first definition for the *lognormal* PDF, following [25] or formula (14.2) in [26], is

$$f(x:m,\sigma) = \frac{1}{x\sigma\sqrt{2\pi}} \exp \frac{-\left[\ln(x/m)\right]^2}{2\sigma^2}. \tag{31}$$

Its average value, $E(m,\sigma)$, is

$$E(m,\sigma) = m\, e^{\frac{\sigma^2}{2}}, \tag{32}$$

and its distribution function, $F(x:m,\sigma)$,

$$F(x:m,\sigma) = \frac{1}{2} - \frac{\operatorname{erf}\left(\frac{\sqrt{2}\left(\ln(m)-\ln(x)\right)}{2\sigma}\right)}{2}. \tag{33}$$

The second definition is

$$f\left(x:\mu,\sigma\right)=\frac{1}{x\sigma\sqrt{2\pi}}\exp\frac{-\left(\ln x-\mu\right)^2}{2\sigma^2}, \tag{34}$$

where $m=\exp\mu$ and $\mu=\ln m$. The average value, $E\left(\mu,\sigma\right)$ is

$$E\left(\mu,\sigma\right)=\mathrm{e}^{\frac{\sigma^2}{2}+\mu}, \tag{35}$$

and the distribution function, $F\left(x:\mu,\sigma\right)$,

$$F\left(x:\mu,\sigma\right)=\frac{1}{2}+\frac{\operatorname{erf}\left(\frac{\sqrt{2}\left(\ln\left(x\right)-\mu\right)}{2\sigma}\right)}{2}. \tag{36}$$

4.2. The Solar Flares

A solar flare can defined as a sudden and dramatic release of a huge burst of solar energy through a break in the Sun's chromosphere in the region of a sunspot. A classification can be made in terms of the peak flux at 1-8 Å, see Table 3.

Table 3. Classification of solar flares, adapted from Table 1 in [27].

level	F_X (Watts × m^{-2})
A	$\left[10^{-8},10^{-7}\right)$
B	$\left[10^{-7},10^{-6}\right)$
C	$\left[10^{-6},10^{-5}\right)$
M	$\left[10^{-5},10^{-4}\right)$
X	$\left[10^{-4},\infty\right)$

The duration in time of a solar flare can be deduced from the online version of the Fermi satellite measurements in the $X-\gamma$ region available at https://hesperia.gsfc.nasa.gov/fermi_solar/. Table 4 gives the sample's parameters for the duration. Table 5 gives the parameters of the lognormal's fit as given by Equation (31) and Figure 11 displays such a fit.

Table 4. Parameters of the sample representing the duration of the X-ray solar flares.

Symbol	Meaning	Value (s)
$t_{\min}$	minimum time	1
$t_{\max}$	maximum time	4522
$\overline{t}$	sample's average	602.68
m	sample's median	315
std	sample's standard deviation	722

Table 5. Parameters of the lognormal distribution of the duration for the X-ray solar flares.

Symbol	Meaning	Value (s)
$\overline{t}$	theoretical average	624.38
m	theoretical median	326.14
σ	shape parameter	1.139
std	theoretical standard deviation	1019

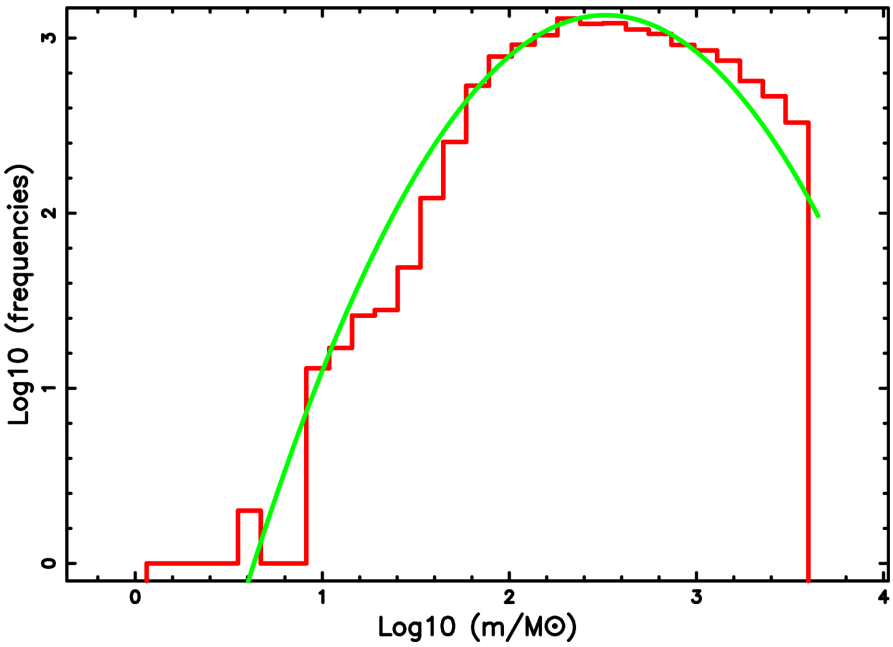

Figure 11. Duration of the the solar X-ray as measured by the Fermi satellite.

4.3. The Electric Field

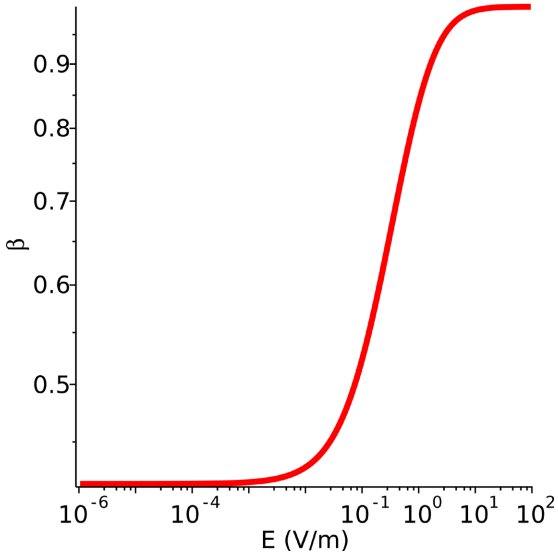

Figure 12. β as function of the electric field when $x = R_{\odot}$ and $x_0 = R_{\odot}/100$, other parameters as in Table 2.

We now briefly review the measurements of the electric field in solar flares. Using the Stark effect exhibited by neutral helium atoms, electric fields with strengths as high as 7×10^4 V m^{-1} were observed [28]. Another measurement of the electric field was done by [29] where field strengths ~50 kV m^{-1} for a limb flare and ~130 kV m^{-1} for a white-light flare were found. In the near-Sun environment a deficit in the sun-ward supra-thermal population of electrons emerges, which is explained by an electric field of ≈ 1 nV/m [30]. The dependence of $\beta = v/c$ on the value of the electric field, see Equation 17 with spatial parameters typical of the solar flares is shown in **Figure 12**.

4.4. Acceleration of Cosmic Rays in Solar Flares

The first mechanism of acceleration for cosmic rays in solar flares was presented by Parker in 1957 [31]. He showed that a 500-gauss field produces a fluid motion of sufficient velocity to accelerate ions from thermal to relativistic energies by Fermi's mechanism in about two minutes. Using the guiding centre approximation, the equation for the acceleration of charged particles is derived from their motion in a magnetic field varying with space and time [32]. The mechanism of collective ion acceleration provides the proton acceleration up to GeV energies in times of 10^{-1} - 10^{-2} s [33]. A non-zero turbulence helicity has a strong effect on the particle acceleration because the helical component of the turbulence induces a mean regular large-scale electric field capable of directly accelerating the charged particles in addition to the commonly considered stochastic turbulent electric field [34]. The highest energies and intensities can be produced in progressive events where shock waves are driven from the Sun by fast and wide coronal mass ejections [35].

5. Conclusions

5.1. The Equation of Motion

We analysed the one-dimensional relativistic motion in the presence of a constant force in the framework of special relativity. Analytical solutions for the acceleration, velocity and the position as a function of time were derived, see Equations (9)-(11). The derivation of the inverse relation between time and position, see Equation (12), allows deriving the velocity as a function of the position when the force due to the electric field is inserted, see Equation (17). The results of the acceleration can also be parametrized in order to have the final kinetic energy expressed as a function of time, see Equation (20). The above discussion answers Question 1 in the Introduction.

5.2. The Simulation

With the parameters given in **Table 2**, the acceleration process by the electric field is working properly in the range $0.1\,\text{GeV} < E_{kin} < 10\,\text{GeV}$ see **Figure 6** and **Figure 9** for the modification introduced on a pre-existing MJ distribution or a gamma-Pareto II distribution. This effect is well explained when the accelerating

effect is expressed in percent as a function of the energy, see **Figure 10**. The above effect explains the absence of the solar modulation of the proton spectra for energies greater than 10 GeV, see figure 25 in [36]. Therefore, the statement that the acceleration in the solar corona affects only the low energy part of the energy spectrum of the CRs, as suggested in Questions 2 and 3 in the Introduction, is justified.

5.3. The Limitations of the Model

The exploration of the electric field in the solar corona, see Section 4.3, has delineated two different regions: one characterized by low values of the electric field, ≈ nV/m, which is referred to as the solar corona, with spherical symmetry, and a second one characterized by high values of the electric field, $\approx 10^4$ V/m, with a cylindrical symmetry. An increase of the observations of the physical parameters such as the density of particles, the temperature, the electric and magnetic fields will allow clarifying the acceleration of CRs in the solar corona as well as in solar flares.

Acknowledgements

The data in Figure 4 and Figure 8 are available at the Cosmic-Ray Data Base (CRDB) or at the Space Science Data Center (SSDC).

Conflicts of Interest

The author declares no conflicts of interest regarding the publication of this paper.

References

[1] Fermi, E. (1949) On the Origin of the Cosmic Radiation. *Physical Review*, **75**, 1169-1174. https://doi.org/10.1103/physrev.75.1169

[2] Fermi, E. (1954) Galactic Magnetic Fields and the Origin of Cosmic Radiation. *The Astrophysical Journal*, **119**, Article 1. https://doi.org/10.1086/145789

[3] Lang, K.R. (1999) Astrophysical Formulae. 3rd Edition, Springer.

[4] Parker, E.N. (1955) Hydromagnetic Waves and the Acceleration of Cosmic Rays. *Physical Review*, **99**, 241-253. https://doi.org/10.1103/physrev.99.241

[5] Davis, L. (1956) Modified Fermi Mechanism for the Acceleration of Cosmic Rays. *Physical Review*, **101**, 351-358. https://doi.org/10.1103/physrev.101.351

[6] Tsytovich, V.N. (1965) Plasma-Turbulence Mechanisms and the Acceleration of Cosmic Rays. *Astronomicheskii Zhurnal*, **42**, 33.

[7] Wentzel, D.G. (1965) Fermi Acceleration of Solar Cosmic Rays. *Journal of Geophysical Research*, **70**, 2716-2719. https://doi.org/10.1029/jz070i011p02716

[8] Fransson, C. and Epstein, R.I. (1980) Acceleration and Propagation of Cosmic Rays. *The Astrophysical Journal*, **242**, Article 411. https://doi.org/10.1086/158474

[9] Voelk, H.J., Drury, L.O. and McKenzie, J.F. (1984) Hydrodynamic Estimates of Cosmic Ray Acceleration Efficiencies in Shock Waves. *Astronomy & Astrophysics*, **130**, 19.

[10] Gieseler, U.D.J., Jones, T.W. and Kang, H. (2000) Time Dependent Cosmic-Ray Shock Acceleration with Self-Consistent Injection. *Astronomy & Astrophysics*, 364,

911. Preprint. https://doi.org/10.48550/arXiv.astro-ph/0011058

[11] Pelletier, G. and Kersalé, E. (2000) Acceleration of UHE Cosmic Rays in Gamma-Ray Bursts. *Astronomy & Astrophysics*, 361, 788. Preprint. https://doi.org/10.48550/arXiv.astro-ph/0007096

[12] Berezhko, E.G. and Taneev, S.N. (2003) Shock Acceleration of Solar Cosmic Rays. *Astronomy Letters*, **29**, 530-542. https://doi.org/10.1134/1.1598235

[13] Niemiec, J. and Ostrowski, M. (2006) Cosmic Ray Acceleration at Ultrarelativistic Shock Waves: Effects of a "Realistic" Magnetic Field Structure. *The Astrophysical Journal*, **641**, 984-992. https://doi.org/10.1086/500541

[14] Orlando, S., Bocchino, F., Miceli, M., Petruk, O. and Pumo, M.L. (2012) Role of Ejecta Clumping and Back-Reaction of Accelerated Cosmic Rays in the Evolution of Type Ia Supernova Remnants. *The Astrophysical Journal*, **749**, Article 156. https://doi.org/10.1088/0004-637x/749/2/156

[15] Podgorny, I.M. and Podgorny, A.I. (2016) Solar Cosmic Ray Acceleration and Propagation. *Sun and Geosphere*, **11**, 85-90.

[16] Taneev, S.N. and Berezhko, E.G. (2020) Solar Cosmic Ray Acceleration at the Front of a Fast Shock in the Lower Solar Corona. *Journal of Experimental and Theoretical Physics*, **131**, 422-431. https://doi.org/10.1134/s1063776120080075

[17] Jüttner, F. (1911) Das maxwellsche gesetz der geschwindigkeitsverteilung in der relativtheorie. *Annalen der Physik*, **339**, 856-882. https://doi.org/10.1002/andp.19113390503

[18] Synge, J. (1957) The Relativistic Gas. North-Holland.

[19] Livadiotis, G. (2016) Modeling Anisotropic Maxwell-jÜttner Distributions: Derivation and Properties. *Annales Geophysicae*, **34**, 1145-1158. https://doi.org/10.5194/angeo-34-1145-2016

[20] Tsouros, A. and Kylafis, N.D. (2017) The Energy Distribution of Electrons in Radio Jets. *Astronomy & Astrophysics*, **603**, L4. https://doi.org/10.1051/0004-6361/201730749

[21] Zaninetti, L. (2020) New Probability Distributions in Astrophysics: IV. the Relativistic Maxwell-Boltzmann Distribution. *International Journal of Astronomy and Astrophysics*, **10**, 302-318. https://doi.org/10.4236/ijaa.2020.104016

[22] Adriani, O., Barbarino, G.C., Bazilevskaya, G.A., *et al.* (2013) Measurement of the Isotopic Composition of Hydrogen and Helium Nuclei in Cosmic Rays with the Pamela Experiment. *Astrophysical Journal*, **770**, 1-9.

[23] Alzaatreh, A., Famoye, F. and Lee, C. (2012) Gamma-Pareto Distribution and Its Applications. *Journal of Modern Applied Statistical Methods*, **11**, 78-94. https://doi.org/10.22237/jmasm/1335845160

[24] Adriani, O., Barbarino, G.C., Bazilevskaya, G.A., *et al.* (2011) Pamela Measurements of Cosmic-Ray Proton and Helium Spectra. *Science*, **332**, 69-72.

[25] Evans, M., Hastings, N. and Peacock, B. (2000) Statistical Distributions. 3rd Edition, John Wiley & Sons Inc.

[26] Johnson, N.L., Kotz, S. and Balakrishnan, N. (1994) Continuous Univariate Distributions. Vol. 1, 2nd Edition, Wiley.

[27] Shao, M., Liu, S., Xu, H., Jia, P., Wang, H., Tong, L., Bai, Y., *et al.* (2025) Advances and Challenges in Solar Flare Prediction: A Review. arXiv:2511.20465.

[28] Davis, W.D. (1977) Measurement of Plasma Wave Electric Fields in Solar Flares. *Solar Physics*, **54**, 139-149. https://doi.org/10.1007/bf00146430

[29] Zhang, Z. and Smartt, R. (1986) Electric Field Measurements in Solar Flares. *Solar Physics*, **105**, Article No. 355. https://doi.org/10.1007/bf00172053

[30] Halekas, J.S., Berčič, L., Whittlesey, P., Larson, D.E., Livi, R., Berthomier, M., *et al.* (2021) The Sunward Electron Deficit: A Telltale Sign of the Sun's Electric Potential. *The Astrophysical Journal*, **916**, Article 16. https://doi.org/10.3847/1538-4357/ac096e

[31] Parker, E.N. (1957) Acceleration of Cosmic Rays in Solar Flares. *Physical Review*, **107**, 830-836. https://doi.org/10.1103/physrev.107.830

[32] Sakurai, K. (1965) On the Acceleration Mechanisms of Solar Cosmic Rays in Solar Flares. *Publications of the Astronomical Society of Japan*, **17**, 403-411. https://doi.org/10.1093/pasj/17.4.403

[33] Fiorentini, G. and Gershtein, S.S. (1993) A Fast Mechanism for the Acceleration of Solar Cosmic Rays and Solar Energetic Particles in Solar Flares. *Physics Letters B*, **307**, 128-131. https://doi.org/10.1016/0370-2693(93)90201-r

[34] Fleishman, G.D. and Toptygin, I.N. (2013) Stochastic Particle Acceleration by Helical Turbulence in Solar Flares. *Monthly Notices of the Royal Astronomical Society*, **429**, 2515-2526. https://doi.org/10.1093/mnras/sts518

[35] Reames, D.V. (2025) Solar Particle Acceleration. *Astronomy*, **4**, Article 5. https://doi.org/10.3390/astronomy4010005

[36] Potgieter, M. (2013) Solar Modulation of Cosmic Rays. *Living Reviews in Solar Physics*, **10**, Article No. 3. https://doi.org/10.12942/lrsp-2013-3